A practical guide to quantify cell adhesion using single-cell force spectroscopy

Jens Friedrichs [a,*], Kyle R. Legate [c], Rajib Schubert [b], Mitasha Bharadwaj [b], Carsten Werner [a], Daniel J. Müller [b,*], Martin Benoit [c,*]

[a] Leibniz Institute of Polymer Research Dresden, Institute for Biofunctional Polymer Materials, Hohe Str. 6, 01069 Dresden, Germany
[b] ETH Zürich, Department of Biosystems Science and Engineering, Mattenstr. 26, CH-4058 Basel, Switzerland
[c] LMU Munich, Applied Physics, Amalienstrasse 54, 80799 Munich, Germany

ARTICLE INFO

ABSTRACT

Quantitative analysis of cellular interactions with the extracellular environment is necessary to gain an understanding of how cells regulate adhesion in the development and maintenance of multicellular organisms, and how changes in cell adhesion contribute to diseases. We provide a practical guide to quantify the adhesive strength of living animal cells to various substrates using atomic force microscopy (AFM)-based single-cell force spectroscopy (SCFS). We describe how to control cell state and attachment to the AFM cantilever, how to functionalize supports for SCFS measurements, how to conduct cell adhesion measurements, and how to analyze and interpret the recorded SCFS data. This guide is intended to assist newcomers in the field to perform AFM-based SCFS measurements.

1. Introduction

Adhesive interactions of cells with their environment trigger signaling pathways that are involved in regulating important cellular processes including cell migration, gene expression, cell survival, tissue organization, and differentiation [1,2]. Accordingly, mutations in genes encoding adhesion receptors [3,4], or adhesion-associated components [5–7] can cause developmental disorders and disease. Consequently, methods that enable the characterization of cell adhesion are pertinent for cell biological, clinical, pharmaceutical, biophysical, and biomaterial research as well as for tissue engineering and regeneration.

Because of the central importance to the above processes, a variety of assays to characterize cell adhesion have been established. Of these assays, single-cell force spectroscopy (SCFS) methods are best able to directly quantify cell adhesion forces from the cellular level down to the contribution of single molecules [8–10]. In this Methods article we will provide a brief overview of the most common methods applied to characterize cell adhesion, mainly focusing on atomic force microscopy (AFM)-based SCFS (AFM–SCFS). We will describe the technical basis of AFM–SCFS with emphasis on clear descriptions of experimental procedures and pitfalls, and will also describe in detail how AFM–SCFS data should be evaluated and analyzed. The background information will enable researchers to understand the principles underlying AFM–SCFS as well as the possibilities and limitations of the method in the quantification of cellular interactions.

1.1. Methods used to characterize cell adhesion

Insight into mechanical interactions between cells and their environment can be gained using different artificial cell culture substrates. Evidence that motile cells exert compressive forces on culture substrates was supplied by the observation that fibroblasts introduce wrinkles into thin silicone rubber film substrates [11]. Based on the stiffness of the substrate and the length of the microscopic wrinkles, the forces exerted by cells can be estimated on the order of nanonewtons (nN) [12]. To detect local deformations, the spatial resolution of this wrinkling substrate approach was

improved by embedding micrometer-sized beads into the substrate [13]. Other studies demonstrated that dynamic deformations of various other substrates was the result of contractile and adhesive cellular forces [14,15]. Although these substrate-based methods have proven important in the understanding of mechanical interactions of cells with their environment, they do not directly provide information about the adhesion strength of cells with substrates.

Methods for examining cell adhesion strength generally focus on measuring the ability of cells to remain attached when exposed to a detachment force. The most common adhesion assay, the plate-and-wash assay, relies on seeding cells onto substrates of interest, washing off "non-adherent" cells with physiological buffers, and counting the remaining cells [16]. Plate-and-wash assays have enabled the identification of key adhesion components and generated valuable insights into mechanisms regulating adhesion [17–19]. However, these assays provide no information on adhesion strength and report only the initial rate of attachment of cells to the substrate as the formation of >10 receptor–ligand bonds is sufficient to prevent their removal from the plate [20].

Several semi-quantitative adhesion assays have been developed to apply controlled shear stress to adherent cells (Table 1). In flow chamber assays, shear stress is exerted to cells by a homogenous buffer flow [21]. In spinning-disc assays, both controlled centrifugal forces and shear flow generated by rotation are applied to cells [22]. Both assays are reported to provide reproducible and controllable results. However, these techniques have limitations since the resistance of cells to detachment by flow and centrifugal forces depends not only on the number, distribution and strength of the adhesion bonds formed, but also on the spread area and surface topography of these cells. Therefore the adhesive strength of the cells to the substrate can only be estimated.

To quantitatively determine the interaction forces of cells with given substrates, sensitive SCFS assays are used (Table 1). SCFS assays allow adhesive interaction forces and binding kinetics to be measured in physiologically relevant conditions from the cellular level down to the contribution of single molecules. In micropipette-based manipulation assays a single cell, held through suction pressure at the tip of a micropipette, is brought into contact with an adhesive surface and subsequently retracted to measure the adhesive forces that have been established. Several micropipette-based experimental techniques that operate both at cellular and molecular levels have been developed including the step pressure technique [23], the biomembrane force-probe [24] and the micropipette aspiration technique [25]. These methods were applied to study surface receptor expression, membrane tether formation

Table 1
Overview of different SCFS assays.

Assay	Type of force application	Read-out	Pro/Contra	References
Plate-and-wash assay	Uneven/unknown shear force	Ratio of attached/non-attached cells	+ Economic + Simple − Low reproducibility − No quantitative data − Relative measure of initial adhesion only	[77–79]
Spinning –disc assay	Shear forces (linear force gradient)	Disc radius at which 50% of the cells remain attached (shear forces estimated)	+ High reproducibility + High throughput + Wide applicable force range − No exact force quantification − Shear forces cell-shape dependent − Not commerciably available	[22,80]
Flow chamber	Shear force (laminar flow)	Ratio of attached / non-attached cells Analysis of rolling cells (binding frequency, arrest time)	+ Simple setup + Commercially available + Widely applicable force range − No exact force quantification − Shear forces cell shape dependent	[81–84]
Centrifugation assay	Shear force (centrifugal force)	Ratio of post-spin to pre-spin cells	+ High reproducibility + High throughput + Wide applicable force range − Shear forces cell shape dependent − Multiple runs at different speeds required − Not commecially available	[77,85,86]
Step pressure technique	Pulling force(suction)	Cell detachment at certain suction pressure	− Restricted to high forces − Low force resolution − Cell shape changes during aspiration	[23,87]
Biomembrane force-probe	Pulling force	Detachment force (0.1 pN–1 nN)	+ High force resolution + Good temporal control − Cell shape changes during aspiration	[24,87,88]
Optical tweezers	Pulling force	Detachment force (0.1–200 pN)	+ High force resolution − Complex experimental setup − Restricted to low detachment forces	[27,89]
AFM–SCFS	Pulling force	Cell detachment force (10 pN–100 nN)	+ High force resolution + Large range of applicable forces + Good control of contact conditions + Commercially available − Time and cost intensive	[9,90,91]

from single cells and single molecule or bond dynamics [26]. The disadvantage of these micropipette-based techniques is either low force resolution (nN range; step pressure technique) or low detectable forces (from $\approx$10 pN to $\approx$1 nN; biomembrane force-probe) Optical tweezers, which trap nano- or micrometer-sized particles in the center of a laser focus, can in principle be employed to study cell-substrate interactions [27,28], but this method is restricted because of the difficulty of measuring forces higher than 100 to 200 pN. Among all of these assays, AFM-based SCFS (from hereon SCFS) is currently the most versatile method to study adhesive interactions of cells with other cells, proteins, and surfaces. This is because SCFS offers a large range of detectable forces, from 10 pN to $\approx$100 nN and offers precise spatial ($\approx$1 nm to $\approx$100 μm) and temporal ($\approx$0.1 s to >10 min) control over the adhesion experiment and the experimental parameters [9]. In the following section we will describe the principles of SCFS in detail.

1.2. Development and applications of SCFS

Initially, AFM-based single-molecule force spectroscopy (SMFS) was used to study the interaction of isolated receptors attached to the AFM cantilever, with ligand-decorated surfaces [29] as well as to measure the interaction of cantilever-linked ligands with receptors bound to a supporting surface [30]. For these SMFS experiments the tip of the AFM is modified with a ligand (or receptor) of interest, then the tip is approached until the ligand (or receptor) on the tip binds to the receptor (or ligand) attached to the supporting surface. After a certain contact time the tip is withdrawn to rupture the receptor–ligand bond. The rupture force is detected by the deflection of the AFM cantilever to which the tip is attached. The same principle of measurement is applied to quantify local receptor–ligand interaction forces on a cellular surface [31]. Based on this design principle, a SCFS setup was developed where the overall adhesion of the cantilever to an immobilized cell was measured [30]. However, this setup has some limitations (see Section 1.3). To overcome these limita-

tions, an inverted SCFS setup was developed [8] (Fig. 1A). In the inverted SCFS setup, a living cell is attached to an AFM cantilever, thereby converting the cell into a 'probe'. Then, the interactions of this 'cellular probe' with a given sample can be quantified [32–34].

For more than a decade, SCFS has been developed and applied as a tool to quantify cell adhesion [8,9,35,36]. Pioneering experiments from the Gaub group revealed for the first time the adhesion strength between two cells of *Dictyostelium discoideum* to single-molecule resolution [8]. Later, Puech et al. identified key proteins regulating the differential adhesive behavior of zebrafish mesendodermal progenitor cells to fibronectin, thereby providing insight into germ layer formation and separation [34]. In a subsequent study the adhesion between gastrulating zebrafish cells derived from different germ layers was quantified [36]. In this way mechanisms underlying cellular sorting during gastrulation could be investigated and the contribution of differential cell adhesion and cell cortex tension in germ layer organization could be deciphered. In a different set of experiments, the $\alpha_2\beta_1$-integrin-mediated adhesion of Chinese hamster ovary (CHO) cells to nanoscopically structured collagen type I matrices was characterized using a combination of knock-out and blocking strategies [10]. In another cell biological study the role of the integrin activator TPA in strengthening integrin-cytoskeleton interactions and increasing $\alpha_2\beta_1$-integrin avidity was monitored [37]. These and other examples [9] highlight the applicability of SCFS to observe the dynamic strengthening of cell adhesive bonds. Characterizing how cells form adhesion starting from the initial binding of individual cell adhesion molecules to their clustering and adhesion strengthening is of particular importance to understand how cells establish and regulate adhesion [10,38–41]. However, the spatial assembly of, for example, ECM molecules also plays a role in cell adhesion, spreading and differentiation [42]. In this respect, the group of Spatz investigated the importance of molecular spacing in modulating adhesion strength by measuring the force required to harvest an adhering cell from a nanopatterned surface by an
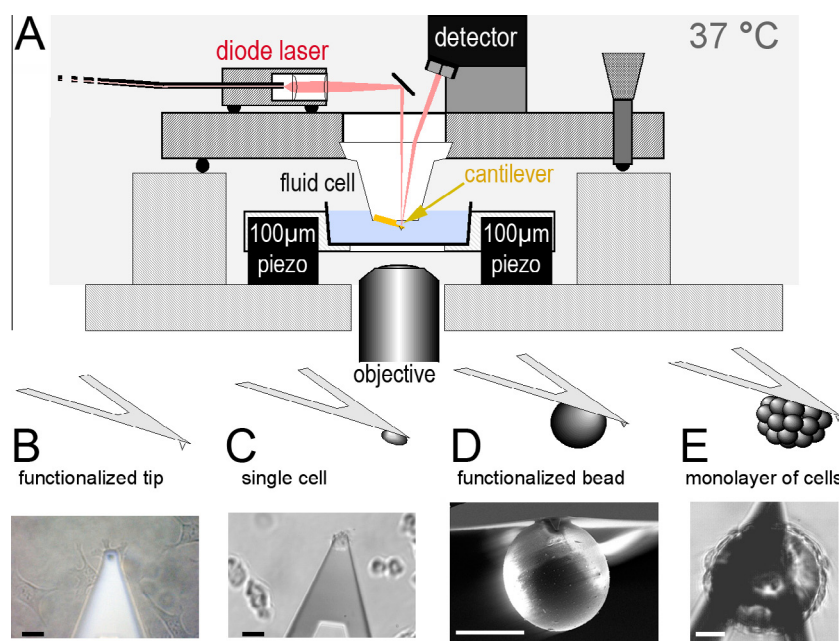

Fig. 1. Experimental setup of AFM-based SCFS and of functionalized cantilevers. (A) To detect the deflection (force) of a functionalized cantilever (see B) a laser is reflected from the cantilever onto a position sensitive photodiode. To bring the cantilever probe into contact with a target cell or substrate, which is present on a cell culture dish, a piezoelectric scanner vertically moves the cell culture dish by at least 100 μm. The setup is mounted onto a light microscope (i.e., phase contrast, DIC, fluorescence, confocal microscope) to optically characterize the cell. The entire setup is preferably placed into a temperature controlled ($\approx$37 °C) and noise isolated chamber. (B) Light microscopy image of endothelial cells probed by a functionalized AFM tip. (C) Single dictyostelium cell attached to a tipless cantilever. The dictyostelium 'probe' cell on the cantilever is placed above other dictyostelium cells plated on a Petri dish. (D) Electron microscopy image of an AFM cantilever that has been functionalized with a micrometer sized bead. The bead can be functionalized with chemical groups or cells to characterize adhesion to a target cell. (E) Monolayer of bone cells cultivated on a bead. Scale bars, 20 μm.

adhesive cantilever [43]. Together, these studies clearly show the versatility of applying SCFS to the investigation of different aspects of cell adhesion.

1.3. Experimental configurations for SCFS

As mentioned earlier, there are two basic configurations for SCFS measurements, which differ in the relationship between cell and cantilever:

(a) A cell adhered to a substrate is contacted by a functionalized tipless AFM cantilever (alternatively a pointed tip or a micrometer sized bead can be used) for a defined contact time and is then retracted from the cell (Fig. 1B and D) [31,44].

(b) A cell adhered to an AFM cantilever is brought into contact with functionalized substrates for a defined contact time and then is retracted from the substrate (Fig. 1C and E).

Configuration (a) has the advantage of testing one type of cantilever functionalization on several cells and thus decreases the influence of outlier cells. However, there are various disadvantages to this approach. First, cellular contacts often leave behind remnants that can contaminate the functionalized tip and thus lose the specificity of the probed interaction (Fig. 2) [45,46]. Consequently, for long-term cell contacts this method obtains just one reliable force measurement. In the case of highly structured cell surface topographies (filopodia, microvilli, microridges, lipid rafts) the matching of the geometry of the tip surface (pyramid, cone, sphere) with the local geometry of the cell surface has a strong influence on the effective surface area interacting between the tip and cell and thus on the measured adhesive forces. Finally, adherent cells differ greatly in their spread area and polarization status, which can have significant effects on the local density and identity of surface receptors. Plating cells onto defined micropatterned substrates can overcome the variability in spreading and polarization, but the possibility of cantilever contamination remains. For these reasons, this configuration is not an option for gaining many reliable data points, particularly for long term contacts. Nevertheless, for short and weak contacts this approach can help to map local adhesion spots on cells [31]. A special application of this configuration is the harvesting of adherent cells by addressing a cell with a cantilever that has greater affinity for the cell than the cell to the substrate [43]. This special format allows for the study of cell adhesion over time points ranging from minutes to hours prior to the detachment measurement.

Configuration (b) has the advantage that the same cell can be probed to different surfaces and in particular to different spots of the same surface to overcome the problem of contamination from cell remnants left behind from prior adhesion events. Provided the cell is not allowed to spread on the cantilever, this configuration also eliminates differences in cell area and

polarization. Disadvantages of this configuration are the additional procedure of immobilizing a cell to the cantilever and the possibility of influencing the state of the cell via the adhesive contact to the functionalized AFM cantilever (see Sections 2.3.2 and 2.4) [47]. Furthermore, single cells can be in different states and thus show distinct adhesive properties that can be difficult to compare. This fact requires that the state of the cells is controlled as tightly as possible by ensuring a homogeneous preparation protocol for each cell type and state, and, the collection of many measurements from different cells to obtain an 'average' adhesion response.

A special application of configuration (b) is the examination of cell–cell adhesion by approaching a second cell or cell layer as a substrate. Advantages of cell–cell measurements are the perfectly prepared surfaces, with respect to the orientation, functionality and natural environment of the interacting molecules. However, cells tend to interact via many molecules of various kinds, thus masking the signal arising from the interaction of interest. Furthermore, variable responses from two cells, rather than only one, contribute to increased variability in the collected data. Nevertheless, for some experiments these exact cellular contributions are the subject of investigation.

In the following sections we aim to discuss the minimal requirements for a SCFS setup to enable the collection of reliable cell adhesion data, with emphasis on configuration (b). We discuss the instrumental and experimental setup, surface modification, cell handling and characterization, cell attachment to the cantilever, conducting the experiments, and data acquisition and analysis.

2. Materials and methods

2.1. AFM and optical microscopy requirements

The minimal requirement for SCFS is an AFM with an extended vertical travel range in order to fully separate a living animal cell from the adherent substrate. To fulfill this criterion it is appropriate to use an AFM that allows vertical movements of up to 100 μm at an accuracy of at least 1 nm. However, to fully separate two adherent animal cells from each other this travel range may easily reach its limits. Unfortunately there is currently no commercially available AFM setup that allows vertical movements larger than 100–120 μm at sufficient accuracy.

The control unit of the AFM used for SCFS should be capable of running a force feedback loop that allows the contact between cell and substrate to be controlled with respect to time and force. SCFS experiments should be conducted in closed loop mode in order to ensure accurate vertical ($\approx$1–10 nm) positioning of the piezoelectric scanner, and thereby accurate and constant movement of the cantilever-immobilized cell with respect to the probed substrate. If closed loop mode is enabled, the piezo position is continuously adjusted and any drift of the positioning system (e.g., creep of the piezoelectric scanner) will be compensated. Vertical drift
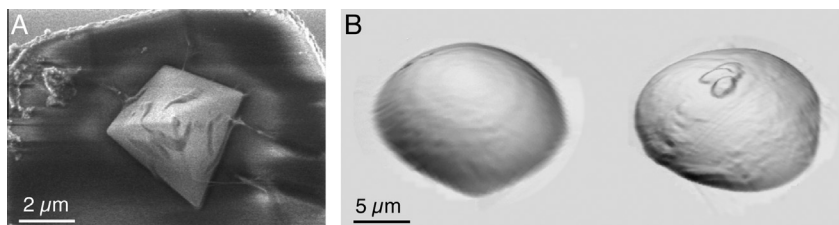

Fig. 2. Cells contaminate tip and bead mounted to the AFM cantilever. (A) Scanning electron microscopy image of an AFM tip after the tip has contacted a living vertebrate cell. The image reveals that the tip surface has been contaminated by microscopic (and possibly also by nanoscopic) fragments from the cell surface. (B) AFM topographs of two beads that have been glued to AFM cantilevers. The left topograph shows the bead before contact with the cell surface. The right topograph shows a bead that has been in gentle contact (applying a force $\approx$2 nN for 5 s) with the surface of a mouse kidney fibroblast and contaminated. SEM image is courtesy of S. Scheuer, LMU Munich.

caused by a thermally or electrically non-equilibrated piezoelectric element in open loop mode can easily push or pull the cell on the cantilever by several hundred nanometers, applying uncontrolled stress to the cell.

During SCFS experiments, the cells under study must be monitored and their morphological details observed. This requires an optical light microscope equipped with objectives that allow structural identification of cells down to a resolution of $\approx$0.5–1 μm (a 20× objective is suitable). Preferably the microscope should allow phase contrast and differential interference contrast (DIC) imaging, and ideally it should have fluorescent imaging options so that fluorescently-labeled cells and cellular structures can be identified. Such extensive light microscopy equipment is of particular importance to guide the initial steps of cell selection and attaching the cell to the cantilever as well as to follow the shape and the functional state of the cell during the experiment and to control the expression level of fluorescently labeled proteins/constructs (see Section 2.4). The shape of the cell can change during the experiment for several reasons. At contact forces above 500 pN the cell becomes squeezed between cantilever and support. Thus the contact area to the support increases. Furthermore, the cell can actively change shape when binding a ligand (or drug). Cells can also actively enforce the adhesion to the cantilever by spreading, it can divide, form blebs or crawl along the sensor surface; all of these events may affect the measured adhesion forces. Therefore, monitoring the cell by light microscopy is mandatory to allow for reliable conclusions and reproducible results.

2.1.1. Reducing thermal drift, vibrational and acoustic noise

Modern AFM devices are sufficiently sensitive to detect the forces required to rupture bonds formed by single receptor–ligand pairs ranging from $\approx$20 to 200 pN. Such sensitivity makes SCFS receptive to thermal drift as well as vibrational and acoustic noise from the environment. Placing the SCFS setup onto a damping isolation table can reduce vibrational noise. Acoustic noise can be reduced by placing the entire system into a sound proof box. Thermal drift can be avoided by either stabilizing the temperature of the room, by using a temperature-controlled sample holder or even better by adjusting the temperature inside the sound proof box.

2.2. Choosing the correct cantilever

For SCFS, soft and tipless AFM cantilevers should be used to prevent perturbation of the cell adhering to the cantilever (recommended cantilevers are e.g. Arrow-TL1 (NanoWorld), PNP-TR-TL-Au (NanoWorld), and NP-O (Bruker)). If tipless cantilevers are not used one must convincingly show that the cell attached to the cantilever is not morphologically constrained by the tip, nor does the tip directly interact with the ligand-coated surface instead of, or in parallel with, the cell. By using fine tweezers, a cantilever with a tip can be truncated to become tipless [48].

To detect single adhesive bonds at the cellular surface (e.g., $\approx$20 to 100 pN), the cantilever spring constants should be as soft as possible ($\approx$10–60 mN/m). In the ideal case the cantilever stiffness should come as close as possible to that of the animal cell investigated (<20 pN/m), to avoid transferring stress to the cell by cantilever movements that are too fast to be compensated for by the feedback system. Most cantilevers are made from silicon or silicon nitride. The latter cantilevers are softer and are therefore preferred for SCFS measurements. Due to their poor reflectivity, silicon nitride cantilevers are usually gold-coated on the backside to improve the reflection of the laser beam detecting the cantilever deflection. This gold-coating, however, makes the cantilever more responsive to small temperature changes. Accordingly, gold-coated cantilevers exhibit enhanced thermal drift and thermal equilibration of the SCFS system takes a considerable length of time.

Another disadvantage of using gold-coated silicon nitride cantilevers is that they tend to undergo significant deflection upon exposure to light intensities used for fluorescence microscopy. In most cases this deflection makes it impossible to simultaneously collect data in the form of force-distance (F–D) curves and fluorescence images of the cells unless specialized techniques such as total internal reflection fluorescence (TIRF) microscopy are used, in which the fluorescent beam does not interact with the cantilever. To circumvent the problems of drift and deflection due to fluorescence beam exposure uncoated silicon cantilevers (e.g. Arrow TL-1 (NanoWorld)) or silicon nitride cantilevers coated with gold on both sides (e.g. PNP-TR-TL-Au (NanoWorld)) should be used.

2.2.1. Cantilever calibration

The deflection of an AFM cantilever is measured by the position of the reflected laser on a photodetector. Accordingly, the units of measurement are volts. To convert the units to a biologically meaningful readout in units of newtons it is necessary to determine the cantilever sensitivity and spring constant. Most manufacturers specify a nominal spring constant for a given cantilever. Usually, the spring constant is calculated using the cantilever shape (length, width, thickness). However, since the true spring constant of a cantilever frequently differs from nominal values by a factor of up to 3, it should always be determined empirically. In the following we provide a quick protocol of how to calibrate a cantilever: First, the cantilever sensitivity is determined from a F–D curve recorded by pressing the cantilever (without cell) on a stiff surface. When cantilever and reference surface are in contact, the deflection of the cantilever is proportional to the vertical movement of the AFM piezo element. Next, the spring constant of the cantilever (without cell) is determined. Most AFM software provides an option to measure the thermal fluctuations (noise) of the cantilever and apply the equipartition theorem to calculate the cantilever spring constant [49]. Essentially, the theorem equates the thermal energy at a given temperature with the energy within the oscillation of the cantilever. The thermal noise method is the most versatile and implementable method of cantilever calibration [50]. A high estimate of the method's error is 20%, which is much smaller than the deviation within one set of SCFS data [50]. It can be argued that other calibration methods are more accurate, but the extra efforts required to apply these with the numerous cantilevers used for SCFS studies make them unfeasible.

2.3. Functionalizing surfaces

2.3.1. Substrate functionalization

Measuring specific adhesion to a substrate requires a functionalized support. Simple procedures have been developed to covalently or non-covalently attach biological or synthetic molecules (e.g., receptors, ligands, peptides) to glass surfaces [10,34,51–53]. After each functionalization procedure it must be carefully proven whether the functionalization was successful, for example by fluorescence imaging. However, optical imaging can only ensure to the resolution limit of the fluorescence microscope ($\approx$0.5–1 μm) whether this coating is homogeneous. Therefore, high-resolution ($\approx$10 nm) AFM imaging may be helpful to image the support and to ensure that the functionalizing molecule covers the supporting surface homogeneously. If doubt still exists whether the imaged surface indeed represents the functionalizing molecule, the AFM tip can be used to scratch squares into the surface coating [54]. In this case the depth of the scratched square should correlate to the thickness of the molecule functionalizing the support.

To enable cell attachment to the cantilever from a non-functionalized surface and subsequent adhesion to substrates of interest within the same dish, it is helpful to coat the surface in a defined region with the ligand of interest, followed by passivation

of the remainder of the surface with a non-adhesive substrate (e.g. BSA). In this way, cells can be attached to the cantilever from a non-adhesive region of the dish, and then relocated to an adhesive region to collect measurements (see Sections 2.4 and 2.5).

2.3.2. Choosing an appropriate cantilever functionalization procedure

In order to attach a cell to the AFM cantilever the cantilever has to be functionalized with a cell-adhesive substrate. Examples of adhesive reagents are CellTak (a formulation of "polyphenolic proteins" extracted from the marine mussel, *Mytilus edulis*, which it uses to anchor itself to solid structures in its natural environment) [55]; lectins such as concanavalin A and wheat germ agglutinin, that specifically recognize sugar groups in the glycocalyx [10,35,56]; antibodies that specifically recognize desired target motifs on a cell surface [53]; DNA [53]; poly-lysine, that due to its positive charge adheres nonspecifically to negatively charges on cells (e.g. to the glycoproteins of their glycocalyx); or ECM proteins that are well recognized by most animal cells e.g. collagens, laminins, and fibronectin [41,47]. It is important to note that the immobilization of a cell, in particular by ECM proteins, lectins or certain antibodies, may have an impact on its adhesive behavior, since ligation or immobilization of certain cell surface receptors might cause activation and signaling [57,58]. For example, it is well known that concanavalin A, commonly used to immobilize fibroblasts and epithelial cells to cantilevers, is a potent activator of immune cells, and must be avoided when working with these cells [59,60]. In many cases simple physisorption is sufficient to functionalize the AFM cantilever. In some cases physisorption may sterically hinder or inactivate the adhesive reagent. In these cases, the presentation of the adhesive reagent on the cantilever must be controlled. The cantilevers can, for example, first be functionalized by physisorption of biotin-BSA, followed by the binding of strepavidin. Finally, biotinylated adhesive reagents can be bound to the cantilevers [61,62].

2.4. Importance of controlling the cell state

In SCFS, emphasis should be placed on maintaining the native state of the cell attached to the cantilever. Cells can show very different adhesive behavior depending on their state [63]. Thus, to obtain a comparable set of experimental data the state of the cells characterized by SCFS should be precisely monitored and controlled. Cells, even from the same established line, are individuals and can react subtly to environmental changes [64]. Moreover, the cellular behavior can also depend on the history of the individual cell. Thus, all cells characterized within one set of SCFS experiments should be cultured and treated in exactly the same way. In particular, cell culture, cell media, phase of the cell cycle, feeding and starving periods, the moment of cell harvesting and transfer to the SCFS measurement, and the application of additional reagents has to be precisely controlled. Even after considering all these experimental parameters cultured cells can expose heterogeneous populations, which affect the outcome of the SCFS experiment. To circumvent this problem cell cultures should be regularly checked by fluorescence activated cell sorting (FACS) for their expression level of, for example, the adhesion proteins targeted by SCFS. Here the selection of cell populations showing a homogeneous expression level of the target proteins can significantly reduce the variability of the SCFS experiment.

2.5. Attaching a cell to the cantilever

For cell attachment, a candidate cell is identified under the microscope, and the functionalized cantilever is aligned such that the end of the cantilever is positioned over the cell. The cantilever is then gently brought into contact with a single cell on a non- or weakly-adhesive surface and is withdrawn as soon as the cell adheres to cantilever. The entire process is monitored by light microscopy (e.g., phase contrast, DIC) to allow a precise positioning of the cantilever above the cell and more importantly to control the cell morphology before and after attachment to the cantilever. Once attached to the cantilever and withdrawn the cell is allowed to firmly attach to the cantilever ($\approx$5–15 min depending on the cell type and state) (Fig. 3A, step 1).

2.6. Recording cell-substrate interactions

After attaching a cell to an AFM cantilever the 'cellular probe' can be used to measure specific or unspecific adhesion to a substrate. Note that the cantilever shall not be removed from the liquid, since most cells will be detached by the surface tension of the air-water interface. The cell is positioned over a region of the support that is functionalized with a ligand of interest, and the cell is then brought into contact with the substrate until a predefined contact force is reached (Fig. 3A, step 2). After a given contact time the cantilever with the cellular probe is retracted from the substrate. If adhesive interactions have been established between the cellular probe and the ligand, the cantilever is deflected downwards during retraction (Fig. 3A, steps 3 and 4). The degree of deflection corresponds to the quantity and strength of the adhesive bonds that have been established between the cellular probe and the substrate. Once the restoring force of the deflecting cantilever exceeds the strength of the interactions between cellular probe and substrate, the cellular probe starts to detach. During cell detachment, the contact zone between cellular probe and substrate shrinks until the cell is fully separated from the substrate (Fig. 3A, steps 4 and 5). While approaching and retracting the cellular probe, the forces acting on the cantilever and the cell-surface distance are recorded in a F–D curve (Fig. 3B). Given that both specific and non-specific adhesion contribute to the F–D curve, an important control experiment should comprise inhibitor experiments to establish the degree of non-specific adhesion. Function blocking antibodies, small molecule inhibitors, or an excess of soluble ligand may be used to block the specific receptor–ligand interaction, resulting in the establishment of a baseline non-specific contribution to the adhesion force.

Measuring the parameters of individual bonds depends less on the contact area than on the contact time and the contact force: The shorter the contact time and the lower the contact force, the fewer bonds can be formed between the receptors and their ligands and the more probable is the measurement of just one single bond. For example, if the adhesion rate is below 30% the probability that the measured bond results from a single molecular interaction is close to 90% [8]. For longer contact times and higher contact forces the probability of multiple bonds contributing to adhesion in parallel increases. In addition to adhesive forces between the cell and substrate, additional information can be collected. By employing very slow retraction velocities or maintaining the cantilever in contact with the surface, even active rearrangements of the cellular cortex will be detected by the AFM [38].

2.7. Apparent versus real changes of cell adhesion

Cell adhesion is dominated by the cell, the cellular environment, and by the experimental SCFS parameters. Increasing the contact time of the cell interacting with the substrate generally leads to increased adhesion. This is regulated by the cell which increases the number and strength of adhesive bonds over time. Increasing the contact force between cell and substrate presses the cell onto the substrate, which increases the contact area and, thus, cell adhesion. Because these two parameters, contact time and force, can strongly influence cell adhesion it is important to control them in each
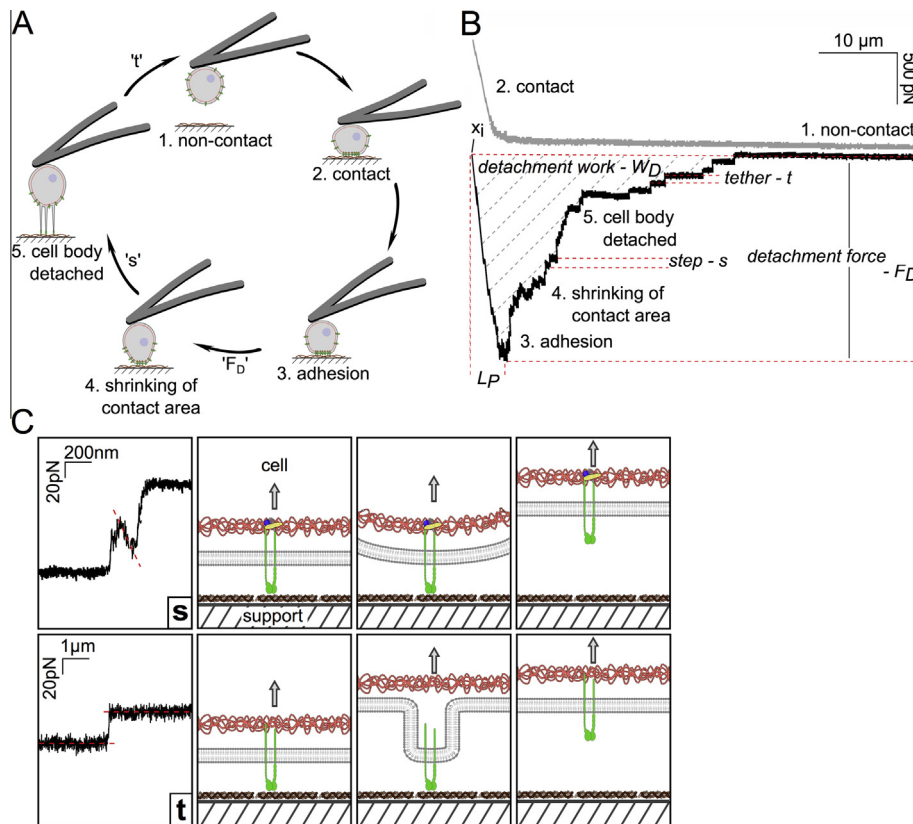
Fig. 3. Schematic illustration of a SCFS experiment and of the adhesion events detected. (A) A single cell is attached to an AFM cantilever (1) and approached to a substrate (1 2). Once in contact, cell adhesion molecules (green) diffuse into the contact zone (2). The adhesive strength between cell and substrate increases. After a predefined contact time, the cell is retracted and the cantilever bends because of the adhesive strength between the cell and the subtrate (3). One the restoring force of the cantilever exceeds the strength of the interactions between cell and substrate, the cell starts to detach (3 4). The force detected at this point corresponds to the maximum detachment force (F_D). During further retraction of the cantilever, the contact area between cell and substrate shrinks (4) and the cell sequentially detaches from the substrate (5) until cell and substrate are completely separated (1). (B) Force-distance (F–D) curve showing steps (1–5) corresponding to those outlined in A. During approach (gray line) and retraction (black line), the force excerted on the cantilever, which is proportional to cantilever deflection, is recorded in a F–D curve. The retraction F–D curve is characterized by the maximum detachment force (F_D). This force is generally followed by step-like events that correspond to the unbinding single cell adhesion molecules from the substrate (s and t events). (C) Illustration of the different processes causing s and t events. s event (upper panel). A cell adhesion receptor (green) anchored to the cytoskeleton (red) binds to a ligand within the ECM (here collagen). Upon cantilever retraction, the cell adhesion receptor-membrane-cytoskeleton linker is stretched and the force on the cantilever increases. Upon bond rupture the force acting on the cantilever rapidly decreases. t event (lower panel). A receptor that is not anchored to the cytoskeleton is extracted at the apex of a membrane nanotube (tether) from the cell body. The force on the cantilever remains constant during tether extraction. When the cell adhesion receptor–ligand bond fails, the force on the cantilever decreases in staircase-like manner.

experiment. Furthermore, the heterogeneous geometry and visco-elastic properties of cells can lead to variable contact areas despite identical contact force and contact time. Therefore, adhesion values between different cells can differ because of variable cell radii and cytoskeletal stiffnesses. Even within a cell line variations in size or elasticity can occur, in particular if the cells are not synchronized in their cell cycle at the moment of their characterization by SCFS. As there is currently no better solution to these problems the user is encouraged to monitor the cell morphology for anormalities in cell shape and spreading before and during SCFS measurements.

2.8. Sampling rate

Interestingly, Brownian motion (thermal noise) acting on the cantilever competes with the detection of individual bonds since they are both of a similar magnitude. At a low sampling rate, the Brownian noise appears to be reduced, but detection of weak bonds is also reduced. In order to facilitate a minute readout of the signatures of individual bonds from a F–D curve the sampling rate plays a crucial role. In particular if the F–D curves will be subjected to smoothing procedures applying low pass filters, a higher sampling rate helps to restore the signal of interest out of the noise.

3. Data analysis

F–D curves recorded by SCFS (Fig. 3B) can be used to extract manifold biophysical parameters that quantitatively describe cellular mechanics and interactions. In the following we describe how to extract and interpret these parameters. Initially it is useful to 'clean up' the F–D curve. As mentioned above the Brownian motion appears as noise in the resonance frequency regime of the cantilever and needs to be reduced to allow analyzing the cellular force signal. Drift due to chemical, thermal or mechanical instabilities in the SCFS setup appears in the very low frequency range. In most cases, drift can be removed from the F–D curve by subtracting a linefit. This procedure can also be used to shift the F–D curve to the zero force baseline by adding an offset. Baseline correction facilitates accurate determination of several parameters including maximum detachment force (Section 3.2.1) and work of detachment (Section 3.2.3).

3.1. Estimating cellular elasticity from the approach F–D curve

In the approach F–D curve the deformation of the cellular probe and the substrate during contact is recorded (the deformation of the substrate can be neglected in the case of a hard surface, but

can be substantial when the substrate is another cell). From this deformation the Young's modulus (E) of the cellular probe can be estimated, when the cellular probe contacts a hard surface. In the case that the contact area between the cell and substrate is large and the deformation of the cell is small (<10% of cell diameter) the Hertz-model can be used [65,66]. Elastic moduli for many cell types have been calculated [67] and they vary over a wide range, but note that the value of the elastic modulus can differ significantly based on whether the Hertz model is used or another model is applied [68]. Algorithms to derive the elastic parameters are widely home made but are also available from different companies and AFM manufacturers.

3.2. Analysing the retraction F–D curve

Sequential and/or parallel rupture of bonds established between the cell and surface, viscous and elastic deformation of the cell body as well as the cell membrane and all molecules encountering the force contribute to the retraction F–D curve. Analysis of the F–D curves was previously restricted to the detection of the maximum adhesion force and the manual determination of the number and magnitude of step-like events. Recently interdisciplinary, home made and commercial algorithms for step detection [69,70] and F–D curve analysis have been developed to make the extraction of adhesion-specific parameters from these curves possible (Fig. 4).

3.2.1. Detachment force
The retraction F–D curve is characterized by a peak adhesion force referred to as the maximum *detachment force* (F_D) with re-

Fig. 4. Principles of AFM-based SCFS experiment after short and weak contact. A HEK 293 cell bound to a PLL coated tipless cantilever (14 pN/nm) pulls a ≈4 μm long tether after interacting with a fibronectin coated surface for 20 ms at 100 pN. (A) raw data disordered by drift and viscous drag. The numbers represent typical stages in the experiment: 1: approaching the surface (in green), 2: forced contact, followed by the retrace (in blue) 3: the zero force level is reached 4: the cell is elongated by adhesive forces 5. A membrane tether has formed and detaches after 4 μm extension. (B) viscous drag and drift were compensated, the dashed base line represents the zero force level. The black circle at position x_i of the retrace force curve represents the zero force of cell and substrate being in contact. The black line is the smoothed retrace force curve. The position of the tether rupture (force step) is indicated by the black arrow. The red cross indicates the detected step of the tether rupture at a force $F_S^t = 28$ pN and position $L_S^t = 4.13$ μm. From the area between the retrace and the zero force level the work of adhesion $W_D = 10.9 \cdot 10^{-15}$J is calculated.

spect to the zero force level. A distance (L_P) can be measured from the point x_i of the initial cell-substrate contact at zero force to the point of maximum adhesion force (Fig. 3B).

3.2.2. Adhesion rate
An *adhesion rate* can be defined as the fraction of F–D curves with at least one detected force step with a peak force greater than a reasonable threshold.

3.2.3. Work of detachment
The *work of detachment* (W_D) describes the energy dissipated during a detachment force experiment by integrating the area of detachment between the zero force level and the contour of the F–D curve (Fig. 3B). The number of receptor–ligand bonds, the stretching of the cell body during retraction (deformation) and the number and length of membrane tethers (see below) contribute to the total amount of detachment work. Note that although this work of detachment is a measurement of energy, there is no trivial relation to the adhesion energy of the involved adhesion molecules.

The maximum detachment force, the work of detachment and the adhesion rate characterize the overall adhesion of a cell, but the following parameters derived from F–D curves focus on the individual bonds involved in the detachment process.

3.2.4. Analysis of discrete unbinding events
The maximum detachment force F_D is typically followed by step-like events, which are either preceded ('s' events) or not preceded ('t' events) by a ramp-like change in force (Figs. 3B and C). These events are attributed to the unbinding or destruction of adhesive units (individual or small aggregates of receptors or cell fragments) from the substrate. In the case of 's' events, adhesive units are connected to the cell cortex [10], whereas for 't' events adhesive units have been extracted from the cortex at the tip of a membrane tether [35]. Therefore the relative presence of 's' events and 't' events can provide information regarding the intracellular interactions of a receptor (i.e. how tightly integrated it is with the cytoskeleton).

The average number of unbinding events detected per curve (only counting curves with at least one detected unbinding event), *number of steps* (N_S), can be split into (N_S^s) and (N_S^t) with respect to the kind of unbinding event ('s' or 't'). The step-like 's' and 't' events are described by either their *absolute step force* ($F_S^{0\,s}$ and $F_S^{0\,t}$), their force with respect to the baseline, or by their *relative step force* (F_S^s and F_S^t) describing the difference in force measured before and after a detachment event, and by their *step position* (L_S^s and L_S^t) with respect to their distance from the point of the initial cell-substrate contact (Fig. 4). The step position is transformed into a *lifetime* (t_B) when dividing the event position by the constant velocity of the retracting cantilever. This is of great interest in the case of 't' events that facilitate a force clamp (see Section 3.3) [71]. The magnitude of the 's' events reflects the stochastic survival of receptor–ligand bonds under an increasing force load [72,73]. The ensemble of 's' events can provide information on the affinity and avidity of cell adhesion receptors.

We emphasize that the step height of the rupture force of a tether cannot simply be seen as an exact measure of the strength of an individual receptor–ligand bond. A force step of an individual bond measured between solid surfaces (support and cantilever) anchored on well known spacers, in general will perform different from the same bond probed by SCFS for several reasons: The cell represents an unknown (sometimes active) spacer, and a membrane tether tunes the measured force step to a plateau force defined by the mechanics of the membrane (see Section 3.3). Thus, the rupture force of the tether does not depend on the strength of the receptor–ligand bond anchoring the tether. Therefore, when
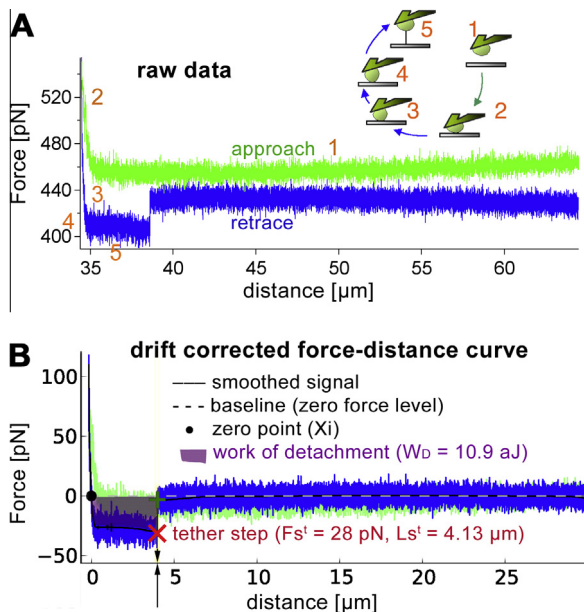
the tether ruptures it will remain unclear how many bonds had anchored the tether before rupture. If two independent membrane tethers are pulled in parallel their plateau forces will add up, but the measured step height might be diminished by the second tether if they pull a common membrane protrusion from the cell. Therefore only the last step to the zero force level measures the true force step of a tether.

3.3. Membrane tethers provide information on membrane and receptor properties and bond lifetimes

Membrane tethers are of great interest for SCFS because they reflect the adhesive state of the cell [74]. Upon applying mechanical stress to a single cell surface receptor the linkage between the receptor and the actomyosin cortex, if there is any, can break and the receptor and membrane are mechanically pulled from the cell surface. The pulling causes the membrane to form tubes a few nanometers in diameter, so-called membrane tethers. Further extracting the membrane tether from the cell surface requires a constant force until the lipid membrane reservoir of the cell membrane is drawn to close. However, the constant tether force (F_s^t) can be described by the membrane tension T_m and membrane stiffness B_m:

$$F_s^t = 2\pi \sqrt{(B_m * T_m)}$$

Hence the tether force reflects the mechanical properties of the cell membrane, which is determined by the composition of lipids and membrane proteins, and how they are anchored to the actomyosin cortex [74]. If a receptor–ligand bond is present at the end of a membrane tether, this bond is loaded by the constant tether force (F_S^t) for a certain time t until the bond breaks. During extraction from the cell membrane tethers dissipate energy ($F_S^t \cdot * \cdot t$) and prevents the bond(s) from becoming loaded at higher force. Thus, the receptor–ligand bond does not rupture because the stressing force is too high, rather the bond fails because the constant force has been applied for too long. This exposure of the bond to a constant force over a long time will increase the likelihood that the bound state crosses the energy barrier towards the unbound state. Thus, membrane tethers apply a native force clamp to the receptor–ligand bond that is in first approximation defined by the properties of the cell membrane. If the number of bonds tethering the membrane is known, the force clamp applied by cell membrane tethers can be used to determine the lifetime of the bond (t_B) under constant force (F_S^t) [75,76]. This approach of using the force clamp innate to the cell membrane allows one to explore the lifetime and the transition state of cell adhesion bonds [71].

In the case of 't'-steps the step height will reach a plateau force – as discussed above. The position/lifetime of the bonds consequently increases with contact time and contact force. The relation of 't'- to 's'-steps cannot be tuned by the AFM parameters and depends on the cell type and the functional state of a cell.

3.4. Statistical analysis

Because cells are individual and complex biological systems, they can differ substantially in their adhesion – even though cell treatment, preparation and conduction of the experiment is identical. Therefore a statistically significant number of measurements has to compensate for this uncertainty. As outlined above, several parameters can be derived from SCFS measurements and from one long adhesion measurement a large number of steps can be analyzed from one F-D curve with respect to height, position and slope while the detachment force will remain a single parameter.

Some experiments in particular use short contact times (e.g. [10]) at low contact forces. Here, a larger number of force curves per cell can be obtained but some F-D curves will not show any adhesion. As many data points as possible should be collected from as many cells as possible for significant results. Plotting the results in histograms will allow one to decide if a Gaussian distribution allows application of a *T*-test or if log-normal distributions or even other distributions with outliers hint for non-parametric statistical analysis (e.g. Mann–Whitney).

4. Conclusions

Like other SCFS techniques, AFM–SCFS suffers from the drawback that each single-cell experiment is time consuming and that acquiring a statistically significant amount of experimental data is time consuming. However, the advantage of AFM–SCFS over other techniques lies in the expanded dynamic range, in which forces can be accurately measured over a couple of orders of magnitude. The complexity of cellular systems requires that a sufficiently large number of cells is collected to derive an 'average', and control experiments must be designed to isolate a specific adhesive interaction from the plethora of non-specific interactions that can contribute to the overall cell adhesion. Despite the challenges inherent in AFM–SCFS experiments, the large amount of information contained within a F-D curve that describes the status of the cell's adhesive machinery renders AFM–SCFS an extraordinarily powerful tool for understanding of how cells establish and control adhesion. The information within the F-D curve contains additive contributions of many cellular properties including cell stiffness, cytoskeletal dynamics, lipid membrane composition, specific receptor–ligand interactions, and non-specific interactions of the glycocalyx. To date the specific contributions of each of these properties to the F-D curve are poorly defined, and better controls and model systems are required to fully understand the contribution each cellular property makes to the overall F-D curve. A future challenge will be to clearly and unambiguously identify each adhesive feature of a cell detected in AFM–SCFS and attribute it to a specific molecular event. In so doing, AFM–SCFS will allow us to obtain a large amount of essential cell biological and biophysical information that will contribute to biomedical and materials applications.

References

[1] K.R. Legate, S.A. Wickström, R. Fässler, Genes Dev. 23 (2009) 397–418.
[2] G.F. Weber, M.A. Bjerke, D.W. DeSimone, J. Cell Sci. 124 (2011) 1183–1193.
[3] R. Fässler, E. Georges-Labouesse, E. Hirsch, Curr. Opin. Cell Biol. 8 (1996) 641–646.
[4] D. Sheppard, Matrix Biol. 19 (2000) 203–209.
[5] S.J. Monkley, X.H. Zhou, S.J. Kinston, S.M. Giblett, L. Hemmings, H. Priddle, J.E. Brown, C.A. Pritchard, D.R. Critchley, R. Fässler, Dev. Dyn. 219 (2000) 560–574.
[6] E. Montanez, S. Ussar, M. Schifferer, M. Bösl, R. Zent, M. Moser, R. Fässler, Genes Dev. 22 (2008) 1325–1330.
[7] J.J. Dowling, E. Gibbs, M. Russell, D. Goldman, J. Minarcik, J.A. Golden, E.L. Feldman, Circ. Res. 102 (2008) 423–431.
[8] M. Benoit, D. Gabriel, G. Gerisch, H. Gaub, Nat. Cell Biol. 2 (2000) 313–317.
[9] J. Helenius, C.-P. Heisenberg, H.E. Gaub, D.J. Muller, J. Cell Sci. 121 (2008) 1785–1791.
[10] A. Taubenberger, D.A. Cisneros, J. Friedrichs, P.-H. Puech, D.J. Muller, C.M. Franz, Mol. Biol. Cell 18 (2007) 1634–1644.
[11] A.K. Harris, P. Wild, D. Stopak, Science 208 (1980) 177–179.
[12] K.A. Beningo, C.-M. Lo, Y.-L. Wang, Methods Cell Biol. 69 (2002) 325–339.
[13] T. Oliver, K. Jacobson, M. Dembo, Methods Enzymol. 298 (1998) 497–521.
[14] K. Burton, D.L. Taylor, Nature 385 (1997) 450–454.

[15] J. Lee, M. Leonard, T. Oliver, A. Ishihara, K. Jacobson, J. Cell Biol. 127 (1994) 1957–1964.
[16] R.J. Klebe, Nature 250 (1974) 248–251.
[17] M. Amano, K. Chihara, K. Kimura, Y. Fukata, N. Nakamura, Y. Matsuura, K. Kaibuchi, Science 275 (1997) 1308–1311.
[18] A.J. Ridley, A. Hall, Cell 70 (1992) 389–399.
[19] D.J. Sieg, C.R. Hauck, D. Ilic, C.K. Klingbeil, E. Schaefer, C.H. Damsky, D.D. Schlaepfer, Nat. Cell Biol. 2 (2000) 249–256.
[20] D. Boettiger, B. Wehrle-Haller, J. Phys. Condens. Matter 22 (2010) 194101.
[21] G. Kaplanski, C. Farnarier, O. Tissot, A. Pierres, A.M. Benoliel, M.C. Alessi, S. Kaplanski, P. Bongrand, Biophys. J. 64 (1993) 1922–1933.
[22] A.J. García, P. Ducheyne, D. Boettiger, Biomaterials 18 (1997) 1091–1098.
[23] K.L. Sung, L.A. Sung, M. Crimmins, S.J. Burakoff, S. Chien, Science 234 (1986) 1405–1408.
[24] E. Evans, K. Ritchie, R. Merkel, Biophys. J. 68 (1995) 2580–2587.
[25] E.A. Evans, R. Waugh, L. Melnik, Biophys. J. 16 (1976) 585–595.
[26] J.Y. Shao, R.M. Hochmuth, Biophys. J. 71 (1996) 2892–2901.
[27] O. Thoumine, P. Kocian, A. Kottelat, J.J. Meister, Eur. Biophys. J. 29 (2000) 398–408.
[28] D. Choquet, D.P. Felsenfeld, M.P. Sheetz, Cell 88 (1997) 39–48.
[29] E.L. Florin, V.T. Moy, H.E. Gaub, Science 264 (1994) 415–417.
[30] P.P. Lehenkari, M.A. Horton, Biochem. Biophys. Res. Commun. 259 (1999) 645–650.
[31] M. Grandbois, W. Dettmann, M. Benoit, H.E. Gaub, J. Histochem. Cytochem. 48 (2000) 719–724.
[32] M. Thie, R. Röspel, W. Dettmann, M. Benoit, M. Ludwig, H.E. Gaub, H.W. Denker, Hum. Reprod. 13 (1998) 3211–3219.
[33] F. Li, S.D. Redick, H.P. Erickson, V.T. Moy, Biophys. J. 84 (2003) 1252–1262.
[34] P.-H. Puech, A. Taubenberger, F. Ulrich, M. Krieg, D.J. Müller, C.-P. Heisenberg, J. Cell Sci. 118 (2005) 4199–4206.
[35] M. Benoit, H. Gaub, Cells Tissues Organs 172 (2000) 174–189.
[36] M. Krieg, Y. Arboleda-Estudillo, P.-H. Puech, J. Käfer, F. Graner, D.J. Müller, C.-P. Heisenberg, Nat. Cell Biol. 10 (2008) 429–436.
[37] M. Tulla, J. Helenius, J. Jokinen, A. Taubenberger, D.J. Müller, J. Heino, FEBS Lett. 582 (2008) 3520–3524.
[38] C.M. Cuerrier, M. Benoit, G. Guillemette, F. Gobeil, M. Grandbois, Pflugers Arch. 457 (2009) 1361–1372.
[39] J. Friedrichs, J.M. Torkko, J. Helenius, T.P. Teräväinen, J. Füllekrug, D.J. Müller, K. Simons, A. Manninen, J. Biol. Chem. 282 (2007) 29375–29383.
[40] J. Friedrichs, A. Manninen, D.J. Müller, J. Helenius, J. Biol. Chem. 283 (2008) 32264–32272.
[41] C. Selhuber-Unkel, M. López-García, H. Kessler, J.P. Spatz, Biophys. J. 95 (2008) 5424–5431.
[42] B. Trappmann, J.E. Gautrot, J.T. Connelly, D.G.T. Strange, Y. Li, M.L. Oyen, M.A. Cohen Stuart, H. Boehm, B. Li, V. Vogel, J.P. Spatz, F.M. Watt, W.T.S. Huck, Nat. Mater. 11 (2012) 642–649.
[43] C. Selhuber-Unkel, T. Erdmann, M. López-García, H. Kessler, U.S. Schwarz, J.P. Spatz, Biophys. J. 98 (2010) 543–551.
[44] A. Muñoz Javier, O. Kreft, A. Piera Alberola, C. Kirchner, B. Zebli, A.S. Susha, E. Horn, S. Kempter, A.G. Skirtach, A.L. Rogach, J. Rädler, G.B. Sukhorukov, M. Benoit, W.J. Parak, Small 2 (2006) 394–400.
[45] L.A. Culp, B.A. Murray, B.J. Rollins, J. Supramol. Struct. 11 (1979) 401–427.
[46] M. Cohen, E. Klein, B. Geiger, L. Addadi, Biophys. J. 85 (2003) 1996–2005.
[47] J. Friedrichs, J. Helenius, D.J. Müller, Proteomics 10 (2010) 1455–1462.
[48] M. Benoit, H.E. Gaub, Cells Tissues Organs 172 (2002) 174–189.
[49] J. Hutter, J. Bechhoefer, Rev. Sci. Instrum. 64 (1993) 1868–1873.
[50] N. Burnham, X. Chen, C. Hodges, G. Matei, E. Thoreson, C. Roberts, M. Davies, S. Tendler, Nanotechnology 14 (2003) 1.
[51] A. Tinazli, J. Tang, R. Valiokas, S. Picuric, S. Lata, J. Piehler, B. Liedberg, R. Tampé, Chemistry 11 (2005) 5249–5259.

[52] P. Jonkheijm, D. Weinrich, H. Schröder, C.M. Niemeyer, H. Waldmann, Angew. Chem. Int. Ed. Engl. 47 (2008) 9618–9647.
[53] S.C. Hsiao, A.K. Crow, W.A. Lam, C.R. Bertozzi, D.A. Fletcher, M.B. Francis, Angew. Chem. Int. Ed. Engl. 47 (2008) 8473–8477.
[54] A.V. Taubenberger, M.A. Woodruff, H. Bai, D.J. Muller, D.W. Hutmacher, Biomaterials 31 (2010) 2827–2835.
[55] G. Ng, K. Sharma, S.M. Ward, M.D. Desrosiers, L.A. Stephens, W.M. Schoel, T. Li, C.A. Lowell, C.C. Ling, M.W. Amrein, Y. Shi, Immunity 29 (2008) 807–818.
[56] X. Zhang, E. Wojcikiewicz, V.T. Moy, Biophys. J. 83 (2002) 2270–2279.
[57] L.L. Kiessling, J.E. Gestwicki, L.E. Strong, Angew. Chem. Int. Ed. Engl. 45 (2006) 2348–2368.
[58] S. Minguet, E.-P. Dopfer, W.W.A. Schamel, Int. Immunol. 22 (2010) 205–212.
[59] J.M. Dwyer, C. Johnson, Clin. Exp. Immunol. 46 (1981) 237–249.
[60] U. Lippi, M. Schinella, M. Nicoli, P. Bellavite, G. Lippi, Int. J. Clin. Lab. Res. 24 (1994) 41–44.
[61] E. Wojcikiewicz, X. Zhang, V. Moy, Biol. Proc. Online 6 (2004) 1–9.
[62] C.M. Franz, A. Taubenberger, P.-H. Puech, D.J. Muller, Sci. STKE 2007 (2007) pp.l5.
[63] G. Weder, J. Vörös, M. Giazzon, N. Matthey, H. Heinzelmann, M. Liley, Biointerphases 4 (2009) 27–34.
[64] F. Rico, C. Chu, M.H. Abdulreda, Y. Qin, V.T. Moy, Biophys. J. 99 (2010) 1387–1396.
[65] T. Ludwig, R. Kirmse, K. Poole, U.S. Schwarz, Pflugers Arch. 456 (2008) 29–49.
[66] A.H. Klemm, S. Kienle, J. Rheinlaender, T.E. Schäffer, W.H. Goldmann, Biochem. Biophys. Res. Commun. 393 (2010) 694–697.
[67] T.G. Kuznetsova, M.N. Starodubtseva, N.I. Yegorenkov, Micron 38 (2007) 824–833.
[68] T. Ohashi, Y. Ishii, Y. Ishikawa, T. Matsumoto, M. Sato, Biomed. Mater. Eng. 12 (2002) 319–327.
[69] J.W.J. Kerssemakers, E.L. Munteanu, L. Laan, T.L. Noetzel, M.E. Janson, M. Dogterom, Nature 442 (2006) 709–712.
[70] J. Opfer, K.-E. Gottschalk, PLoS ONE 7 (2012) e45896.
[71] M. Krieg, J. Helenius, C.-P. Heisenberg, D.J. Muller, Angew. Chem. Int. Ed. Engl. 47 (2008) 9775–9777.
[72] E.A. Evans, D.A. Calderwood, Science 316 (2007) 1148–1153.
[73] E. Evans, K. Ritchie, Biophys. J. 72 (1997) 1541–1555.
[74] M.P. Sheetz, Nat. Rev. Mol. Cell Biol. 2 (2001) 392–396.
[75] R.M. Hochmuth, H.C. Wiles, E.A. Evans, J.T. McCown, Biophys. J. 39 (1982) 83–89.
[76] R.M. Hochmuth, E.A. Evans, Biophys. J. 39 (1982) 71–81.
[77] A.J. García, N.D. Gallant, Cell Biochem. Biophys. 39 (2003) 61–74.
[78] R.J. Klebe, J.R. Hall, P. Rosenberger, W.D. Dickey, Exp. Cell Res. 110 (1977) 419–425.
[79] W.L. Connors, J. Heino, Anal. Biochem. 337 (2005) 246–255.
[80] N.D. Gallant, A.J. García, Methods Mol. Biol. 370 (2007) 83–96.
[81] E. Martines, K. McGhee, C. Wilkinson, A. Curtis, IEEE Trans. Nanobiosci. 3 (2004) 90–95.
[82] J.J. Zwaginga, K.S. Sakariassen, G. Nash, M.R. King, J.W. Heemskerk, M. Frojmovic, M.F. Hoylaerts, J. Thromb. Haemost. 4 (2006) 2716–2717.
[83] J.J. Zwaginga, G. Nash, M.R. King, J.W. Heemskerk, M. Frojmovic, M.F. Hoylaerts, K.S. Sakariassen, J. Thromb. Haemost. 4 (2006) 2486–2487.
[84] T.G. van Kooten, J.M. Schakenraad, H.C. Van der Mei, H.J. Busscher, J. Biomed. Mater. Res. 26 (1992) 725–738.
[85] R. Burger, J. Ducrée, Expert. Rev. Mol. Diagn. 12 (2012) 407–421.
[86] C.D. Reyes, A.J. García, J. Biomed. Mater. Res. 67 (2003) 328–333.
[87] J.-Y. Shao, G. Xu, P. Guo, Front. Biosci. 9 (2004) 2183–2191.
[88] C. Gourier, A. Jegou, J. Husson, F. Pincet, Cell. Mol. Bioeng. 1 (2008) 263–275.
[89] K.C. Neuman, A. Nagy, Nat. Methods 5 (2008) 491–505.
[90] P.-H. Puech, K. Poole, D. Knebel, D.J. Muller, Ultramicroscopy 106 (2006) 637–644.
[91] J. Friedrichs, J. Helenius, D.J. Müller, Nat. Protoc. 5 (2010) 1353–1361.